ELSEVIER

Journal of Molecular Catalysis A: Chemical 178 (2002) 79–87

JOURNAL OF MOLECULAR CATALYSIS A: CHEMICAL

www.elsevier.com/locate/molcata

Hydrogenolysis of 1,1a,6,10b-tetrahydro-1,6-methanodibenzo[*a*,*e*]cyclopropa[*c*] cycloheptene over Ru-zeolites

Roxana Preda [a], Vasile I. Pârvulescu [a,*], Aurica Petride [b], Anca Banciu [b], Angela Popescu [c], Mircea D. Banciu [c]

[a] *Department of Catalysis, Faculty of Chemistry, University of Bucharest, B-dul Regina Elisabeta 4-12, Bucharest 70346, Romania*
[b] *Center of Organic Chemistry, Splaiul Independentei 202B, P.O. Box 15-258, 71141 Bucharest, Romania*
[c] *Department of Organic Chemistry, Polytechnic University of Bucharest, Splaiul Independentei 313, Bucharest, Romania*

Received 29 November 2000; accepted 11 April 2001

Abstract

Hydrogenolysis of 1,1a,6,10b-tetrahydro-1,6-methanodibenzo[*a*,*e*]cyclopropa[*c*] cycloheptene (**I**) over Ru-beta and Ru-Y zeolites is reported. The catalysts were prepared via impregnation of commercial beta and Y zeolites using $Ru(NH_3)_6Cl_3$, $RuCl_3$ or $Ru(acac)_3$, as precursors. The catalysts were characterized by chemical analysis, adsorption–desorption isotherms of N_2 at 77 K, hydrogen chemisorption and temperature programmed oxidation (TPO). Hydrogenolysis of (**I**) was carried out in methanol or 2-propanol, as solvent, at temperatures in the range 60–100 °C. The reaction was mainly influenced by the type of zeolite and solvent.

Keywords: Hydrogenolysis; Ru-beta and Ru-Y zeolites; 1,1a,6,10b-Tetrahydro-1,6-methanodibenzo[*a*,*e*]cyclopropa[*c*] cycloheptene

1. Introduction

The synthesis of 1,1a,6,10b-tetrahydro-1,6-methanodibenzo[*a*,*e*]cyclopropa[*c*] cycloheptene (**I**) was first achieved by Huang–Minlon reduction of the corresponding dibenzotricyclic ketone [1] and then by elimination during solvolysis of dibenzocycloheptatrienyl-β-ethyl tosylate [2,3]. Later on, this compound was also obtained in flash-vacuum pyrolysis of dibenzocycloheptatrienyl-β-ethanol both in radical (quartz) and cationic (zeolite) conditions [4,5]. The structure of this molecule was fully confirmed by IR [2,3], UV spectroscopy [6], ^{1}H NMR [2,3], and finally X-ray analysis [7].

Since its synthesis, several attempts have been done to use this molecule as a substrate. Among those, hydrogenation over PtO_2 in ethanol at atmospheric pressure was unsuccessful [3]. Hydrogenolysis of this molecule to compounds **II**, **III** or **IV** (Scheme 1) may be an alternative to obtain some interesting synthons for organic syntheses.

Hydrogenolysis is generally known as an unselective reaction in which the pathway is strongly dependent on the metal dispersion [8]. Up to this day, most of these reactions were carried out in gas phase to prove its structural sensitivity character. An acidic support or toxics like Cl may exert an influence on the catalyst selectivity and stability [9]. Informations on the

* Corresponding author. Fax: +40-13-159249.
E-mail address: v_parvulescu@chim.upb.ro (V.I. Pârvulescu).

1381-1169/02/$ – see front matter
PII: S1381-1169(01)00228-X

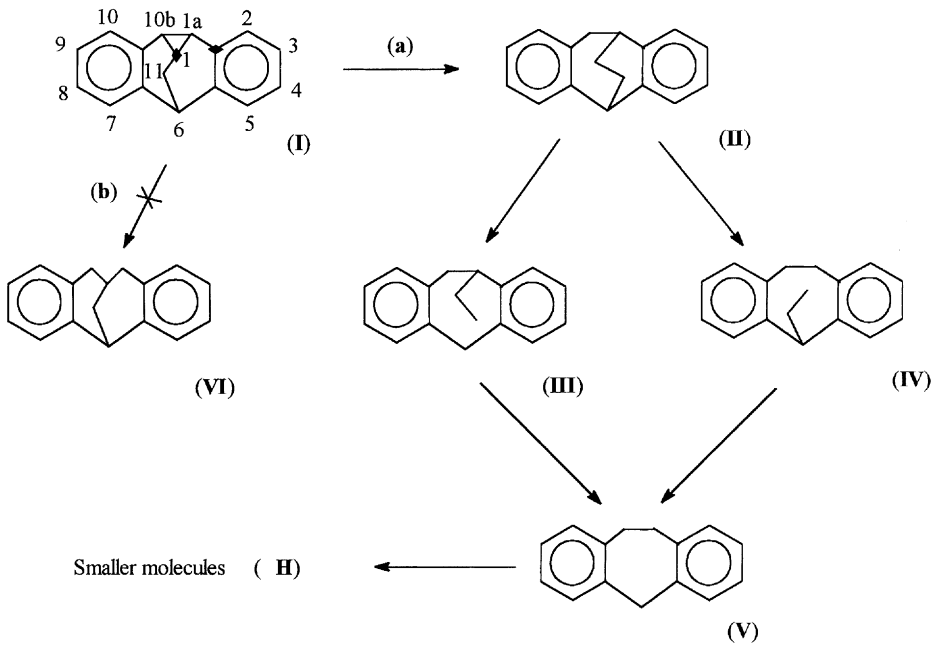

Scheme 1. Routes in hydrogenolysis of (**I**).

hydrogenolysis of the C–C bond at low temperatures and in the liquid phase are scarce.

This paper deals with the hydrogenolysis of (**I**) over Ru supported on two different acid zeolites, beta and Y. In a first step, such a reaction could theoretically follow routes **a** and **b** presented in Scheme 1. In fact, only route (**a**) is operative, leading to (**II**), and then to (**V**) via the intermediates (**III**) and (**IV**). In a following step, compound (**V**) may undergo both hydrogenolysis and hydrocracking to smaller molecules. Therefore, the selectivity of this reaction was another item followed in this study. The aim was to stop the hydrogenolysis at the level of compound (**V**). Derivatives of (**V**) exhibit biological activity. One example is well-known drug elavil [10].

2. Experimental

Ru-beta and Ru-Y were prepared by deposition of Ru from various precursors on commercial beta (SiO_2/Al_2O_3 21.6) and Y (SiO_2/Al_2O_3 5.1) zeolites (Valfor PQ Company). As Ru precursors, $Ru(NH_3)_6Cl_3$, $RuCl_3$, and $Ru(acac)_3$ were used. The deposition of the metal was carried out from an aqueous solution. In the case of $RuCl_3$, the solution was slightly acidified with HCl (35 wt.% solution) while for $Ru(acac)_3$, water was mixed with methanol in a 1:1 volume ratio. After stirring for 72 h, the catalysts were separated, washed with distilled water, and dried under vacuum at room temperature for 24 h. The catalysts were then calcined for 3 h at 350 °C and *reduced for 4 h at the same temperature under a hydrogen flow of* 30 ml min^{-1}. The resulting catalysts were denoted as Ru-HCl (when the precursor was $RuCl_3$), Ru-NH (for $Ru(NH_3)_6Cl_3$), and Ru-acac (for Ru-acac). Table 1 compiles the chemical composition of these catalysts.

Thermal curves (TG-DTA) were recorded using a SETARAM TGA 92.16.18 equipment. The samples in amounts of 40 mg were heated in a high purity air stream (Air Liquide) from ambient temperature until 1000 °C at a heating rate of 10 °C min^{-1}.

H_2-chemisorption measurements were carried out using a Micromeritics ASAP 2010C apparatus. The reduced samples were evacuated, first at 120 °C and then at 450 °C. Soon after, a hydrogen flow was passed initially at 35 °C for 15 min and then the

temperature was increased at 450 °C at a heating rate of 10 °C min^{-1} and maintained for 2 h. After reduction, the samples were purged with a helium flow at 417 °C for 2 h, and at 35 °C for another 30 min. The amounts of chemisorbed hydrogen were measured at 35 °C by the desorption method after equilibration for 45 min in 300 Torr of adsorbate. The total hydrogen uptake was determined by extrapolating the linear portion of the adsorption isotherm to zero pressure. Reversible H_2 sorption was measured by outgassing at 5×10^{-5} Torr at the adsorption temperature and running a second isotherm. The difference between the total and reversible uptakes was ascribed to irreversible hydrogen. The ruthenium dispersion, surface area, and particle size were determined from the irreversible uptake, assuming a H:Ru stoichiometry of 1 [11,12]. The amount of metal considered in the calculation was that determined by O_2 titration performed in TPO conditions on catalysts reduced at 450 °C, using a Micromeritics Pulse Chemisorb 2705 apparatus and a 5 vol.% O_2 in He gas mixture (50 ml min^{-1}). Typical experiments were carried out at 450 °C with a ramp of 10 °C min^{-1}. Reduced ruthenium was determined assuming that at 450 °C ruthenium is converted to RuO_2 [13], an assumption that was confirmed by XPS analysis. The actual fraction of Ru was used to determine the metal dispersion and thereby, to calculate the fraction of the exposed metal atoms.

The XPS spectra were recorded using a SSI X probe FISONS spectrometer (SSX-100/206) with monochromated Al Kα radiation. The spectrometer energy scale was calibrated using the Au $4f_{7/2}$ peak (binding energy 84.0 eV). For the calculation of the binding energies, the C 1s peak of the C–(C, H) component of adventitious carbon at 284.8 eV was used as an internal standard. In order to limit reoxidation, the reduced samples were transferred from the reduction set-up to the XPS apparatus under isooctane. The peaks assigned to the Ru $3p_{3/2}$ and Ru $3d_{5/2}$, Si 2p, and O 1s levels were analyzed. No peak due to a chlorine *compound* was identified.

Standard experiments used 10 mg (**I**) dissolved in 15 ml methanol or 2-propanol and 50 mg catalyst (corresponding to a substrate:catalyst molar ratio of 2:1). The reaction was carried out in a stainless steel stirred autoclave under a pressure of 8 atm and temperatures between 60 and 100 °C. The reaction products were collected each 15 min up to 4 h. The products were analyzed by gas chromatography, using a Carlo Erba instrument (HRGC 5300 Mega Series) equipped with a fused silica capillary column of 25 m length and 0.32 mm inner diameter. The identification of the peaks was made with *pure* compounds (**II**) [2,3] and (**V**) [14], the purity of which was controlled by ^{1}H and ^{13}C NMR, with a Varian Gemini 300B instrument operated at 300 MHz for ^{1}H and 75 MHz for ^{13}C.

3. Results

3.1. Textural measurements

The data presented in Table 1 show that the deposition of ruthenium led to an important decrease of the Langmuir surface area indicating a blockage of the pores. The precursor had an influence in this process. For each zeolite, the surface area decreased in the order Ru-HCl > Ru-NH > Ru-acac. For the beta zeolites, *high t*-plot surface areas were obtained even after the deposition of 5 wt.% Ru.

Table 1
Textural characteristics of the Ru-zeolites

Catalyst	Ru content (wt.%)	Langmuir surface area of parent zeolite (m^2 g^{-1})	Langmuir surface area of Ru-zeolite (m^2 g^{-1})	*t*-plot surface area of Ru-zeolite (m^2 g^{-1})
Ru-HCl-beta	5	738	298	201
Ru-NH-beta	5	738	226	182
Ru-acac-beta	5	738	204	167
Ru-HCl-Y	5	440	115	79
Ru-NH-beta	5	440	108	66
Ru-acac-Y	5	440	87	45

Table 2
Chemisorption and TPO data for the investigated catalysts

Catalyst	Reduction degree (%)	H_2 uptake ($cm^3\ g^{-1}$)	Dispersion (%)	Particle size (nm)	XPS binding energy (eV)
Ru-HCl-beta	48.5	0.5243	5.9	22.6	462.4
Ru-NH-beta	51.3	0.5202	5.8	23.1	462.2
Ru-acac-beta	69.8	0.1855	2.1	63.7	462.0
Ru-HCl-Y	53.2	0.3511	3.9	34.3	462.4
Ru-NH-Y	56.8	0.3319	3.7	36.1	462.3
Ru-acac-Y	74.3	0.1608	1.8	74.3	461.9

3.2. Chemisorption data

The H_2-chemisorption data and the reduction degree determined from TPO are compiled in Table 2. These values were used as a basis for the calculation of the chemisorption parameters. The reduction degree was near 70% only for the catalysts prepared from ruthenium acetylacetonate. For the other precursors, the reduction degree was smaller, indicating a stronger interaction with the support. The nature of the ruthenium precursor also influenced the dispersion. For both supports, dispersion decreased in the order, Ru-HCl > Ru-NH > Ru-acac. The metal particle size determined from the same measurements exceeded 20 nm, and reached about 75 nm in the case of Ru-acac-Y. These data confirm the general behavior of Ru to generate, during impregnation, large metal patches on the support.

3.3. XPS

Binding energies of Ru $3p_{3/2}$ component are given in Table 2. They showed minor differences between the catalysts. *The measured values were between those reported for Ru(0) (461.2 eV) and Ru(**IV**) (462.4 eV)* [15,16]. *Although the differences between the binding energies are not significant*these data may confirm the TPO results, which indicated a reduction degree of ruthenium in the range 50–75%.

3.4. Catalytic data

Fig. 1 shows the conversion of (**I**) *after* 4 h over Ru supported on beta and Y zeolites. These data show a higher activity of the Ru-beta catalysts. The analysis of the reaction products indicated the absence of the compounds (**II**)–(**V**) of Scheme 1. The nature of the

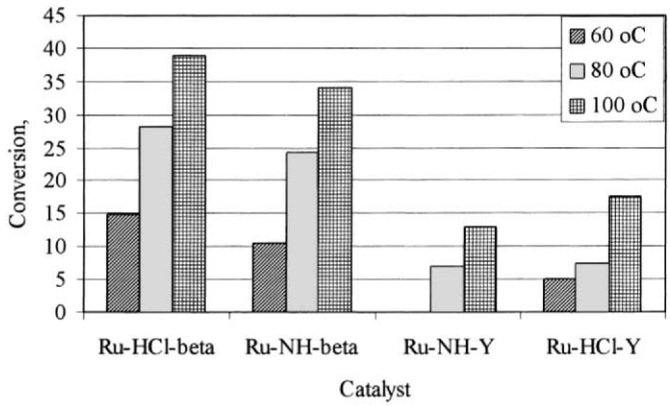

Fig. 1. Conversion of (**I**) on the investigated catalysts (10 ml methanol, 8 atm H_2, 4 h, 50 mg catalyst, 30 mg substrate, 100 °C).

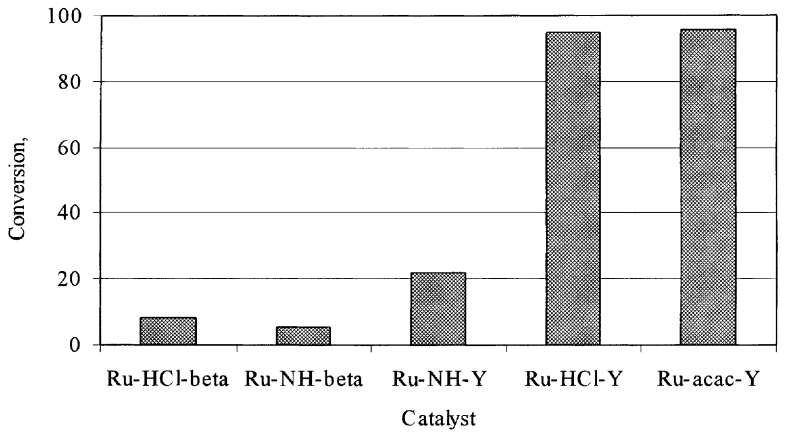

Fig. 2. Conversion of (**I**) over the investigated catalysts in 2-propanol (10 ml 2-propanol, 8 atm H_2, 4 h, 50 mg catalyst, 30 mg substrate, 100 °C).

metal precursor only had a small influence. In this reaction, the catalysts behaved as bifunctional ones, in which the metal sites cooperate with the acidic sites of the support. *The catalytic data suggest* that beta zeolite exhibited stronger acid sites than Y one. Catalytic tests done over Ru-free beta or Y zeolite indicated a rapid deactivation, presumably due to the polymerization of fragments resulting from cracking, with formation of coke. It is worth to mention here that previous work of our group revealed the conversion of (**I**) to benzofluorene derivatives and coke in the presence of zeolite catalysts at 350 °C in flash-vacuum conditions [5]. In all the cases, the increase of the temperature led to an increase of the total conversion.

At 60 °C, hydrogenolysis merely gave compounds (**III**) and (**IV**) in which the bridge is partially broken. The increase of the temperature to 80 and 100 °C, resulted in the increase of compound (**II**) and degradated molecules (**H**). The amount of (**V**) was, however, small irrespective of the reaction conditions. The evolution of the reaction products as a function of temperature may suggest that at higher temperatures, the increasing

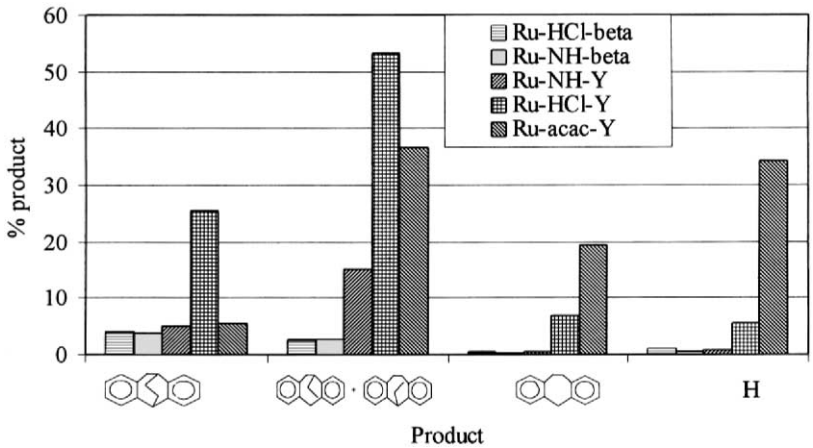

Fig. 3. Product distribution as a function of the investigated catalysts (10 ml 2-propanol, 8 atm H_2, 4 h, 50 mg catalyst, 30 mg substrate, 100 °C).

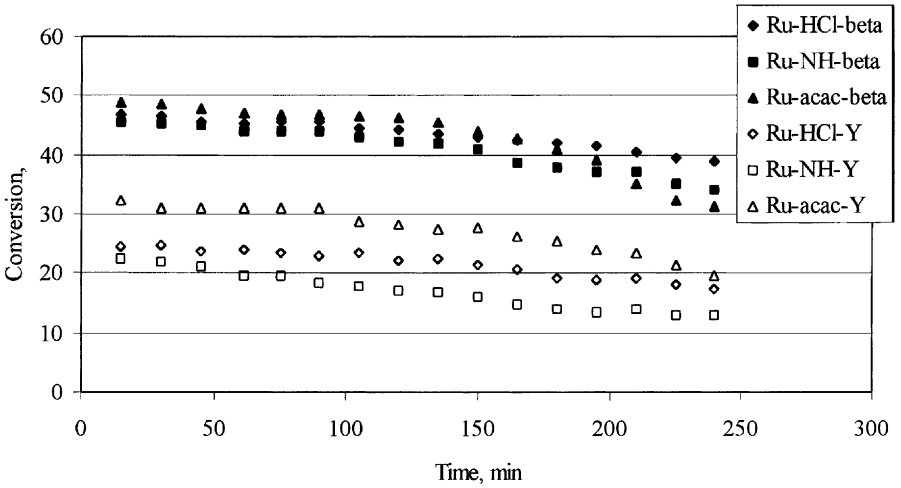

Fig. 4. Time dependence of the conversion (10 ml methanol, 8 atm H_2, 4 h, 50 mg catalyst, 30 mg substrate, 100 °C).

amounts of the products (**H**), which can easily polymerize, lead to the partial poisoning of the active surface and, hence, to a diminution of compounds (**III**) and (**IV**).

Changing the solvent (2-propanol instead of methanol) gave a different picture (Fig. 2). Under such conditions, higher conversions were achieved over the Y zeolites compared with the beta ones. Over Ru-HCl-Y and Ru-acac-Y, the conversion was almost total.

Fig. 3 shows the product distribution using 2-propanol as a solvent. The best selectivities were obtained on Ru-HCl-Y. Over Ru-acac-Y, *there are less compounds (**III**) and (**IV**) and more compounds (**V**) and (**H**) compared with Ru-HCl-Y.*

3.5. Catalysts deactivation

Figs. 4 and 5 show the time dependence of the conversion of (**I**) in methanol and 2-propanol, respectively. "However, the variations presented in these figures gave not a comparative picture of the behavior of various catalysts because the differences in the conversions were rather high". The decrease of the

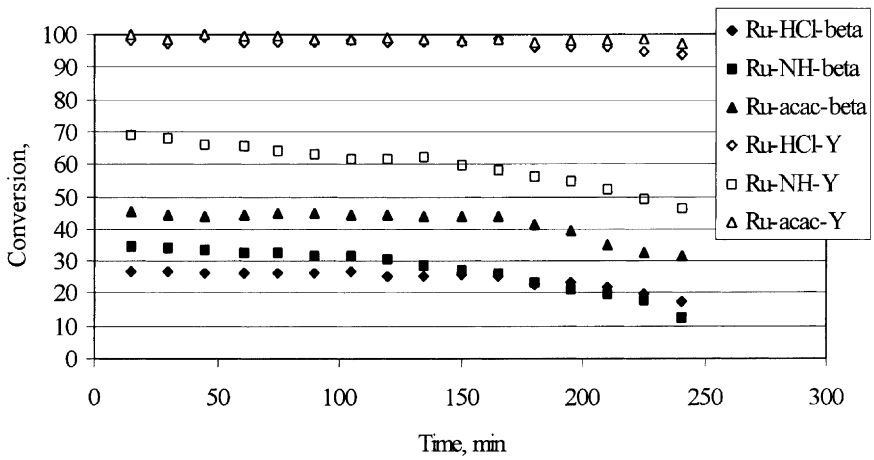

Fig. 5. Time dependence of the conversion (10 ml 2-propanol, 8 atm H_2, 4 h, 50 mg catalyst, 30 mg substrate, 100 °C).

conversion with time is related both to the precursor nature and the solvent in which the reaction is carried out. In methanol, the decrease of the conversion was more evident on Ru-NH and Ru-acac catalysts. In 2-propanol, the behavior of Ru-HCl catalysts was *similar*, but the Ru-acac-Y catalyst also showed a pretty good time stability.

TG-DTA measurements carried out over the catalysts separated after the catalytic tests showed a similar trend as the catalytic data. The amount of the carbonaceous deposits decomposed during heating at 1000 °C were in a perfect proportionality with the decrease of the conversion. *That means that the loss of the mass caused by the burning of the carbonaceous deposits was higher for Ru-NH-beta and Ru-NH-Y reacted in 2-propanol and very small for Ru-HCl-beta and Ru-acac beta tested in the same solvent. The data recorded for the other catalysts were intermediate*.

4. Discussion

The characterization of the catalysts showed that the deposition of ruthenium occurs with the formation of large patches. However, the nature of the ruthenium precursor and *type* of zeolite have an influence on the metal *particle* size. The Ru supported on beta zeolite exhibited higher dispersions and, for each zeolite, the size of the metal *particles* increased in the order, Ru-HCl < Ru-NH < Ru-acac. The reduction degree varied in the reverse order, the Ru-acac samples being the most reduced ones.

Deposition of 5 wt.% ruthenium led to a decrease of the surface area due to pore blockage. The identity of the ruthenium precursor had an influence on this decrease. For both supports, the surface area decreased in the order, Ru-acac > Ru-NH > Ru-HCl. "Data presented in Table 1 indicated that the drop in the Langmuir and *t*-plot surface areas is different. Langmuir surface area decreased for Ru-beta catalysts in the limits 60% (Ru-HCl) to 72% (Ru-acac), while for Ru-Y from 74% (Ru-HCl) to 80% (Ru-acac). The differences between the two zeolites are in agreement with the pore size of these materials, namely 7.6 for beta and 7.0 for Y [17]. The decrease of the *t*-plot surface area accounts to the different texture of the two zeolites. Beta zeolite exhibits an external surface area of about 220 $m^2 g^{-1}$ and Y of about 45 $m^2 g^{-1}$. For beta zeolite, the decrease of the external surface area varied from 8.6% (Ru-HCl) to 24% (Ru-acac) and for Y from 13.3% (Ru-HCl) to 44.4% (Ru-acac). Both the decrease of the Langmuir and *t*-plot surface areas are very well correlated with the Ru-particle size. This varied between 22.6 nm (Ru-HCl) and 63.7 nm (Ru-acac) for beta and between 34.3 nm (Ru-HCl) and 74.3 nm (Ru-acac) for Y, indicating a clear relation between the size of the Ru particles and the decrease of the surface area".

The blockage of the pores may have some positive effects in the case of our substrate. The substrate is unable to penetrate inside the *zeolite porosity*, but the smaller hydrogenolysis products may react on the acid sites inside of the pores leading to carbonaceous deposits. It is worth to note that for the Ru-beta catalysts, the external surface areas determined from the *t*-plot values were still high. For this zeolite, the pore size is however greater than for Y one.

The catalytic data indicated that in the hydrogenolysis of (**I**), the Ru-zeolites act as bifunctional catalysts. The support is far to be inactive in this reaction. The tests done over the Ru-free zeolites as well as previous results [5] indicate that polymerization is the main reaction leading to the catalyst deactivation. Therefore, it is expected that the reaction occurs at the border of the metallic particles with the acidic sites of the zeolites. The bridges, first the cyclopropane (1,1a or 1,10b) and then, the ethano bridges are opened as a contribution of the metal sites. Interestingly, the first step of the hydrogenolysis, namely, the *rupture* of the strained cyclopropane ring occurs regioselectively via route (**a**) (Scheme 1), probably due to the fact that the Cl–H bond being the most unhindered cyclopropanic one, it is most easily fixed on the catalyst and then hydrogenated, giving the hydrocarbon (**II**). In the next steps, part of the resulting fragments migrates to the zeolite where they undergo polymerization while another part is hydrogenated by the metal particles. The dibenzocycloheptanic hydrocarbon (**V**) was undoubtedly identified among the *reaction* products by comparison with a *standard* sample [14].

The experimental data showed important differences according to the solvent used in these reactions. In the investigated range of parameters, the conversion was lower than 40% in the presence of methanol. Under these conditions, the selectivity to (**II**)–(**IV**) predominated and the best results were obtained

over the Ru-beta catalysts. The use of 2-propanol instead of methanol caused a very important increase of the conversion for the Ru-HCl-Y and Ru-acac-Y catalysts although the behavior of these two catalysts was different. Using Ru-acac-Y, the (**H**) species predominated while in the presence of Ru-HCl-Y, hydrogenolysis to species (**II**)–(**IV**) was prevailing. Good selectivities to species (**II**)–(**IV**) were also obtained using Ru-HCl-Y in methanol.

These data show that the solvent was far from inert in this reaction. For both solvents, higher conversions were achieved over the Ru-HCl and Ru-acac zeolites, but in methanol, the best results were obtained with Ru-beta, whereas in 2-propanol, with the Ru-Y zeolites. The behavior of the Ru-acac catalysts is typical of Ru in hydrogenolysis reactions, namely, large metal particles led to a more advanced rupture of C–C bonds [18,19]. The good selectivities obtained over Ru-HCl also account for the well-known relation between the metal particle size of Ru and its rupture capacity.

But the relatively high conversions of (**I**) over the Ru-HCl zeolites are more difficult to explain because this catalyst has the higher dispersion of Ru. XPS analysis of the catalysts surface and the chemical analyses did not show the presence of chlorine. However, some traces may still be present. Therefore, a possible explanation may be those we found for hydrogenolysis of butane on Co-Nb_2O_5-SiO_2 catalysts, when the presence of the acid sites in the close proximity of the metal particles may hinder the self-poisoning of the active sites by the surface reaction products [20]. The traces of chlorine may help this process.

The effect of the solvent is more complicated to explain. The obtained results are very probably the contribution of the interaction of the solvents with the supports. 2-Propanol may relatively easy release hydrogen through a hydrogen transfer reaction. Bekkum and coworkers [21,22] proved that such a reaction may easily occur on beta zeolites (Scheme 2). Under such conditions, it may be speculated that for beta zeolites

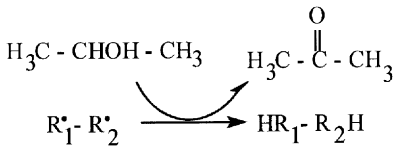

Scheme 2. Inhibiting effect of the hydrogen transfer reaction.

a competition between the two reactions occurs, leading to the low conversions we observed. For the Y zeolites, the accessible free metal surface is smaller and, in the absence of any interaction with the support, the conversions are higher. “These processes should also be related with the differences observed in the external surface areas of the investigated zeolites”. Following these hypotheses, it may be further speculated that the results obtained in methanol are also the consequence of the support. Methanol may be adsorbed on very acidic surface of beta which can hinder the positive effect of the acid sites in the very close proximity of the metal. “The interaction of the alcohols with very acidic surface of these zeolites has been already reported in the literature. Hunger and Horvath [23] have shown that methanol molecules form clusters around the silanol groups, which may have a direct influence on the catalytic reaction”.

Part of the hydrogenolysis products migrates on the support where it undergoes a typical acid catalyzed process. The contribution of this process to the catalysts deactivation from the analysis of the time dependence of the conversion curves or the TG-DTA results is hard to be appreciated, because, at the same time, a deactivation of the metal particles also occurs. However, these curves illustrate the positive effect of the acid sites surrounding small metal particles in keeping a certain level of activity.

5. Conclusions

Hydrogenolysis of compund (**I**) over Ru-supported on beta and Y zeolites occurs as a bifunctional process. The first step of the hydrogenolysis, namely, the breaking of cyclopropane ring, proceeds regioselectively, affording (**II**). The different external surface and acidity of the support have an effect on the polymerization of the fragments formed during the initial steps of the hydrogenolysis. Hydrogenolysis occurs on the metal surface and the nature of the precursor is very important. The solvent also plays a very important role leading to different conversions and selectivities.

References

[1] V. Ioan, M. Popovici, C.D. Nenitzescu, Tetrahedron Lett. (1965) 3383.

[2] E. Cioranescu, M.D. Banciu, R. Jelescu, M. Rentzea, M. Elian, C.D. Nenitzescu, Tetrahedron Lett. (1969) 1871
[3] E. Cioranescu, M.D. Banciu, R. Jelescu, M. Rentzea, M. Elian, C.D. Nenitzescu, Rev. Roum. Chim. 14 (1969) 911.
[4] M.D. Banciu, S. Stan, A. Banciu, A. Petride, C. Florea, Rev. Roum. Chim. 38 (1993) 469.
[5] M.D. Banciu, O. Cira, A. Petride, A. Banciu, C. Draghici, J. Anal. Appl. Pyrolysis 42 (1997) 177.
[6] M.D. Banciu, M.D. Stanescu, C. Florea, A. Petride, C. Draghici, E. Cioranescu, Bull. Soc. Chim. France 128 (1991) 919.
[7] N.G. Furmanova, M.D. Stanescu, M.D. Banciu, Rev. Roum. Chim. 37 (1992) 461.
[8] F. Garin, L. Hilaire, G. Maire, in: L. Cerveny (Ed.), Catalytic Hydrogenation, Elsevier, Amsterdam, Stud. Surf. Sci. Catal. 27 (1986) 145.
[9] V. Ponec, G.C. Bond, Catalysis by Metals and Alloys, Elsevier, Amsterdam, 1995, p. 284.
[10] M. Protiva, V. Hnevsova, M. Seidova, J. Metysova, J. Med. Pharm. Chem. 4 (1961) 411.
[11] T. Komaya, A.T. Bell, Z.W. Sieh, R. Gronsky, F. Engelke, T.S. King, M. Pruski, J. Catal. 150 (1994) 400.
[12] D.O. Uner, M. Pruski, T.S. King, J. Catal. 156 (1995) 60.
[13] P.G.J. Koopman, A.P.G. Kieboom, H. van Bekkum, J. Catal. 69 (1981) 172.
[14] W. Treibs, H.J. Klinkhammer, Chem. Ber. (1951) 84.
[15] J.C. Fuggle, T.E. Madey, M. Steinkilberg, D. Menzel, Surf. Sci. 52 (1975) 521.
[16] A.J. McEvey, W. Gissler, Phys. Status Solid A69 (1982) K91.
[17] W.M. Meier, D.H. Olson, Atlas of Zeolite Structure Types, Butterworth-Heinemann, London, 1992.
[18] J. Schwank, J.-Y. Lee, J.G. Goodwin Jr., J. Catal. 108 (1987) 495.
[19] G.C. Bond, R. Yahya, B. Coq, J. Chem. Soc., Faraday Trans. I 86 (1990) 2297.
[20] V. Pârvulescu, P. Grange, V.I. Pârvulescu, Catal. Today 57 (2000) 193.
[21] E.J. Creyghton, S.D. Ganeshie, R.S. Downing, H. van Bekkum, J. Mol. Catal. A: Chem. 115 (1997) 457.
[22] P.J. Kunkeler, B.J. Zuurdeeg, J.C. van der Waal, J.A. van Bokhoven, D.C. Koningsberger, H. van Bekkum, J. Catal. 180 (1998) 234.
[23] M. Hunger, T. Horvath, Catal. Lett. 49 (1997) 95.